Human Molecular Genetics, 2011, Vol. 20, No. 23 ***4569–4581***
doi:10.1093/hmg/ddr391
Advance Access published on August 31, 2011

Gene therapy using self-complementary Y733F capsid mutant AAV2/8 restores vision in a model of early onset Leber congenital amaurosis

Cristy A. Ku[1,2], Vince A. Chiodo[4], Sanford L. Boye[4], Andrew F.X. Goldberg[5], Tiansen Li[6], William W. Hauswirth[4] and Visvanathan Ramamurthy[1,2,3,*]

[1]Center for Neuroscience, [2]Department of Ophthalmology and [3]Department of Biochemistry, Robert C. Byrd Health Sciences Center, West Virginia University, Morgantown, WV 26505, USA, [4]Department of Ophthalmology, University of Florida, Gainesville, Florida 32610, USA, [5]Eye Research Institute, Oakland University, Rochester, Michigan 48309, USA and [6]N-NRL, National Eye Institute, Bethesda, MD 20892, USA

Received May 27, 2011; Revised and Accepted August 28, 2011

Defects in the photoreceptor-specific gene *aryl hydrocarbon receptor interacting protein-like 1* (*Aipl1*) are associated with Leber congenital amaurosis (LCA), a childhood blinding disease with early-onset retinal degeneration and vision loss. Furthermore, *Aipl1* defects are characterized at the most severe end of the LCA spectrum. The rapid photoreceptor degeneration and vision loss observed in the LCA patient population are mimicked in a mouse model lacking AIPL1. Using this model, we evaluated if gene replacement therapy using recent advancements in adeno-associated viral vectors (AAV) provides advantages in preventing rapid retinal degeneration. Specifically, we demonstrated that the novel self-complementary Y733F capsid mutant AAV2/8 (sc-Y733F-AAV) provided greater preservation of photoreceptors and functional vision in *Aipl1* null mice compared with single-stranded AAV2/8. The benefits of sc-Y733F-AAV were evident following viral administration during the active phase of retinal degeneration, where only sc-Y733F-AAV treatment achieved functional vision rescue. This result was likely due to higher and earlier onset of *Aipl1* expression. Based on our studies, we conclude that the sc-Y733F-AAV2/8 viral vector, to date, achieves the best rescue for rapid retinal degeneration in *Aipl1* null mice. Our results provide important considerations for viral vectors to be used in future gene therapy clinical trials targeting a wider severity spectrum of inherited retinal dystrophies.

INTRODUCTION

Inherited retinal dystrophies are a large group of clinically and genetically diverse conditions estimated to affect 1 in 3000 people (1). The earliest and most severe form is Leber congenital amaurosis (LCA), which is estimated to account for $\geq$5% of inherited retinopathies (2,3). LCA is diagnosed with clinical findings of severely impaired visual function shortly after birth, sluggish pupillary responses, nystagmus and an absent or markedly reduced electroretinogram (ERG). Patients with LCA may also exhibit fundus changes, photophobia, the occulodigital sign, keratoconus and cataract (2,4). To date, LCA is associated with mutations in at least 15 different genes expressed in either photoreceptor or retinal pigment epithelium (RPE) cells (Human Gene Mutation Database, http://www.hgmd.org, last accessed 12-4-11). Clinical heterogeneity within LCA had long been recognized (4–7), but more recent genotype–phenotype correlation studies showed subtle but important differences in fundus appearance, visual acuity and disease progression (8–10).

Greater understanding of the molecular basis of genetic defects in inherited retinopathies coupled with developments in viral-mediated gene delivery have led to potential therapies for some retinal dystrophies, which were a previously untreatable group of diseases. Defects in RPE-specific protein 65 kDa (*RPE65*) are associated with autosomal recessive retinitis

*To whom correspondence should be addressed at: One Stadium Drive, West Virginia University Eye Institute, Morgantown, WV 26505, USA. Tel: +1 3045986940; Fax: +1 3045986928; Email: ramamurthyv@wvuhealthcare.com

pigmentosa and LCA. In multiple animal models, mutations in *RPE65* lead to vision loss but photoreceptor neurons develop normally and survive for an extended period (11–13). This characteristic of *RPE65* mutations was crucial in successful preclinical trials in multiple animal models (14–17). Although patients with *RPE65* mutations exhibit greater photoreceptor degeneration than animal models, optical coherence tomography (OCT) demonstrated preservation of the photoreceptor cell layer that is greater than predicted from the level of visual dysfunction (18). These findings indicated that there is a window of time for therapeutic intervention, which made *RPE65* patients an ideal initial target for gene therapy trials. Landmark clinical trials which delivered exogenous *RPE65* gene using the adeno-associated virus 2 (AAV2), showed visual improvements in patients (19–24), and are paving the way for gene therapy for inherited retinal degenerative diseases associated with other genetic defects.

On the other end of the disease spectrum are mutations linked to LCA that cause rapid photoreceptor degeneration. The degeneration is pronounced when associated with defects in *Aryl hydrocarbon receptor interacting protein-like 1 (Aipl1)*. AIPL1 is a 386-amino acid protein that belongs to the FK506-binding protein family of chaperone proteins (25), and is expressed early and specifically in photoreceptors (26). AIPL1 is crucial for the stability of rod phosphodiesterase 6 (PDE6), an enzyme that is involved in cyclic GMP phototransduction signaling (27–29). Although the role in cone photoreceptors is not fully understood, AIPL1 is required for cone function and survival (30). In the *Aipl1* null mouse, both rod and cone ERG responses are absent and complete photoreceptor cell loss occurs by 3 weeks of age (27). Patients with *Aipl1* mutations, implicated in 5–7% of LCA cases and several incidences of juvenile retinitis pigmentosa and cone-rod dystrophy (31), have a stable but drastically reduced visual acuity by the first decade in life, ranging from 20/200 to no light perception (10,32,33). The level of photoreceptor survival in patients has not been extensively examined, but two recent studies found photoreceptors in OCT scans of patients with mutations in *Aipl1* (34,35). While the window of therapeutic opportunity is smaller in *Aipl1* defects due to rapid photoreceptor degeneration, these findings highlight the possibility that patients with *Aipl1* defects could benefit from early gene replacement therapy.

Two important proof-of-concept studies used AAV-mediated gene replacement therapy in the *Aipl1* hypomorphic and null mouse (36,37). These were the first studies to show that *Aipl1* replacement could restore functional rod and cone PDE6 and prevent the loss of photoreceptors. Since these two studies, advancements in virology resulted in AAV vectors with increased transduction efficiency and shortened onset of expression. The first development was self-complementary AAV, which produces a double-stranded gene vector that is more stable and eliminates the need for second-strand DNA synthesis (38). These characteristics conferred both earlier onset and increased transduction efficiency compared with single-stranded AAV (39–41). The second development was mutations of surface-exposed tyrosine residues on the viral capsid. The resultant decrease in capsid tyrosine phosphorylation reduces ubiquitination of viral particles and subsequently improves nuclear transport and transduction efficiency (42,43).

The aim of this study was to utilize these developments in AAV vectors in order to maximize therapeutic effects of gene replacement therapy for rapid retinal degeneration. Specifically, we assessed the efficiency of gene replacement therapy using single-stranded AAV2/8 (ssAAV) or the novel self-complementary Y733F tyrosine capsid mutant AAV2/8 (scAAV) delivering the human *Aipl1* gene. In these studies, we first assessed the onset and efficiency of gene expression achieved with each virus in wild-type retina. We further evaluated the level of vision rescue that ssAAV or scAAV provides to *Aipl1*−/− mouse, a model of rapid retinal degeneration, following treatment at an early and later stage of photoreceptor degeneration.

RESULTS

Self-complementary AAV capsid mutant induces earlier and higher expression of hAIPL1 in retina

Self-complementary Y733F tyrosine capsid mutant AAV2/8 combines two recent developments in AAV vectors shown to increase transduction efficiency and decrease expression latency of reporter genes (39–41). To compare the onset and levels of expression of single-stranded AAV and self-complementary capsid mutant AAV, we injected ssAAV-RKp-h*Aipl1* (henceforth referred to as ssAAV) or scAAV-Y733F-RKp-h*Aipl1* (henceforth referred to as scAAV) into postnatal day 14 (P14) wild-type retina. Viral titers were matched between ssAAV and scAAV for all experiments throughout this study. The vectors expressed the human *Aipl1* gene under the short rhodopsin kinase promoter (RKp), which is active in both rod and cone photoreceptor cells as early as P2 (44–46). Expression of exogenously delivered human AIPL1 was investigated through immunofluorescent staining of whole mounted injected eyes with an antibody that specifically recognizes the human isoform of AIPL1. Eyes injected with ssAAV exhibited low AIPL1 expression in sparse areas beginning at post-injection (pi) day 3, with progressive increases at pi days 5 and 7. Expression of AIPL1 began to plateau between pi days 7 and 14 (Fig. 1A). In comparison, eyes injected with scAAV exhibited expression of AIPL1 in larger areas beginning at pi day 2 and uniformly high expression at pi day 3. Expression of AIPL1 increased steadily and uniformly at pi days 5, 7 and 14 (Fig. 1A). Fluorescent counts quantifying AIPL1 expression were conducted on three treated retina per post-injection time point. Mean fluorescent counts were significantly higher in scAAV-treated eyes than ssAAV-treated eyes at pi days 3, 5 and 14 ($P < 0.0005$) (Fig. 1B). scAAV-treated retina had a 4-fold higher mean fluorescent count than ssAAV at pi day 3, and a 2-fold difference at pi day 5 and pi day 14. Differences in AIPL1 expression were particularly evident at earlier time points, with expression levels of scAAV at pi day 3 greater than levels of ssAAV at pi day 5.

Early administration of AAV-mediated gene replacement therapy efficiently rescues photoreceptor function in *Aipl1*−/− mice

Aipl1−/− mice exhibit rapid and severe photoreceptor degeneration (27,47), with initiation of cell death at P8

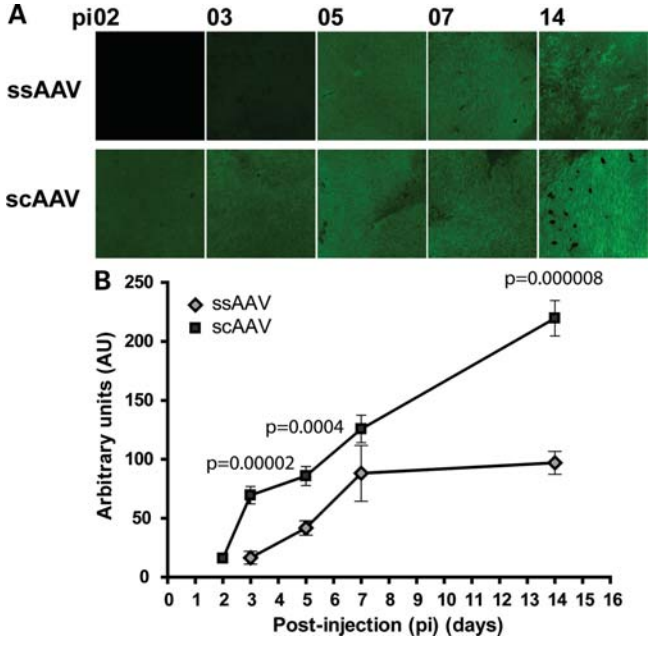

Figure 1. scAAV provides earlier onset and higher expression compared with ssAAV following subretinal injection into wild-type retina. (**A**) Whole mount images from injected retina at indicated post-injection (pi) times. All images were taken with the same exposure time at ×20 magnification. Scale bar, 100 μm. (**B**) Quantitative analysis of AIPL1 expression in whole mount images, expressed in arbitrary units of fluorescence (AU). Except for pi day 7, statistically significant differences in units of fluorescence between ssAAV and scAAV were observed. Error bars, ± SEM.

(Supplementary Material, Fig. S1). In addition, photoreceptor cells in these mice are not functional at any age tested (27). Our goal was to compare the efficacy of ssAAV and scAAV in preventing cell death and in rescuing visual function. Therefore, we injected AAV-h*Aipl1* subretinally into one eye of *Aipl1*−/− mice at P2. At this early stage of retinal development, rod photoreceptors in mice are beginning to form. ERGs, a measure of light-dependent electrical responses from photoreceptor cells and downstream neurons, were conducted to evaluate photoreceptor function after treatment with either ssAAV or scAAV. The *a*-wave in ERG correlates with photoreceptor activity, while the *b*-wave arises mainly due to downstream bipolar cell activity. Representative ERG recordings at P30 under dark-adapted (Fig. 2A) and light-adapted conditions (Fig. 2B) showed restoration of scotopic and photopic ERG responses in ssAAV- and scAAV-treated eyes compared with a complete absence of response in the contralateral untreated eye. The scAAV-treated eye showed greater *a*- and *b*-wave amplitudes and oscillatory potentials than the ssAAV-treated eye at all dark-adapted scotopic flash intensities of −3.6, −1.6, −0.6 and 0.4 log (cd s/m^2) flashes. At a flash intensity of −0.6 log (cd s/m^2), the photoreceptor responses (*a*-wave amplitudes) of individual mice in each treatment group showed intergroup variability (Fig. 2C). However, the mean group average for scAAV was statistically higher than for ssAAV-treated mice ($P = 0.027$; ssAAV treated mean = 49.5 ± 8.7 μV, $n = 10$; scAAV treated mean = 79.5 ± 11.6 μV, $n = 10$). This difference in group means of *a*-wave amplitudes was statistically significant at every scotopic flash intensity recorded (*P*-values indicated in figure, ranging from $P = 0.017$ to $P = 0.027$) (Fig. 2D).

Early administration of AAV-mediated gene replacement therapy restores rod and cone PDE6 expression and slows photoreceptor degeneration in *Aipl1*−/− mice

To evaluate the effects of *Aipl1* replacement on photoreceptor survival, we examined the retinal morphology in AAV-treated and -untreated control eyes. Immunocytochemical and morphometric analyses were conducted at P65 after a single injection at P2. As expected, treated eyes showed expression of hAIPL1 in photoreceptor inner segments and outer plexiform layer (30,37) (Fig. 3A). Concomitant with the expression of hAIPL1, rod and cone PDE6 was observed along with rod and cone opsins, indicating the presence of intact rod and cone outer segments (Fig. 3A). ssAAV-treated eyes showed four to five rows of photoreceptor cell nuclei compared with a complete loss of photoreceptors in the contralateral untreated eye. scAAV-treated retina had five to six rows of photoreceptor nuclei (Fig. 3A, and Supplementary Material, Fig. S2). To quantify the observed differences in outer nuclear layer thickness, photoreceptor cell nuclei counts were conducted on retina from each treatment group. The mean number of photoreceptor cell nuclei of scAAV-treated retina was significantly greater than ssAAV-treated retina by 45% ($P = 0.005$; ssAAV mean = 125.92 ± 14.43; scAAV mean = 182.85 ± 13.42) (Fig. 3B). In agreement with our ERG and morphology results, western blots showed that retina from scAAV-treated animals expressed higher levels of AIPL1 and rod PDE6 than ssAAV-treated animals (Fig. 3C). This trend was also observed when protein levels were examined at P35, where all scAAV-treated animals expressed higher levels of AIPL1 and rod PDE6 (Supplementary Material, Fig. S3) at this earlier post-injection time point.

Early administration of AAV-mediated gene replacement therapy preserves photoreceptor ultrastructure

The effectiveness of AAV-mediated gene replacement therapy on preserving photoreceptor ultrastructure was evaluated through light and transmission electron microscopy. Semi-thin sections showed scAAV-treated retina with longer inner and outer segments compared with ssAAV-treated retina (Fig. 4A). At best, outer segments in ssAAV-treated retina were 40–50% of the length of outer segments in an age-matched wild-type retina, whereas scAAV-treated retina were 50–60% of wild-type retina (Fig. 4A). Additionally, semi-thin sections showed similar findings to immunohistochemical studies in outer nuclear layer thickness, with ssAAV-treated retina with four to five rows of nuclei and scAAV-treated retina with five to six rows (Fig. 4A). Ultrastructurally, both ssAAV- and scAAV-treated retina displayed intact photoreceptor outer segments with normally organized and densely stacked disc membranes, similar to wild-type retina (Fig. 4B).

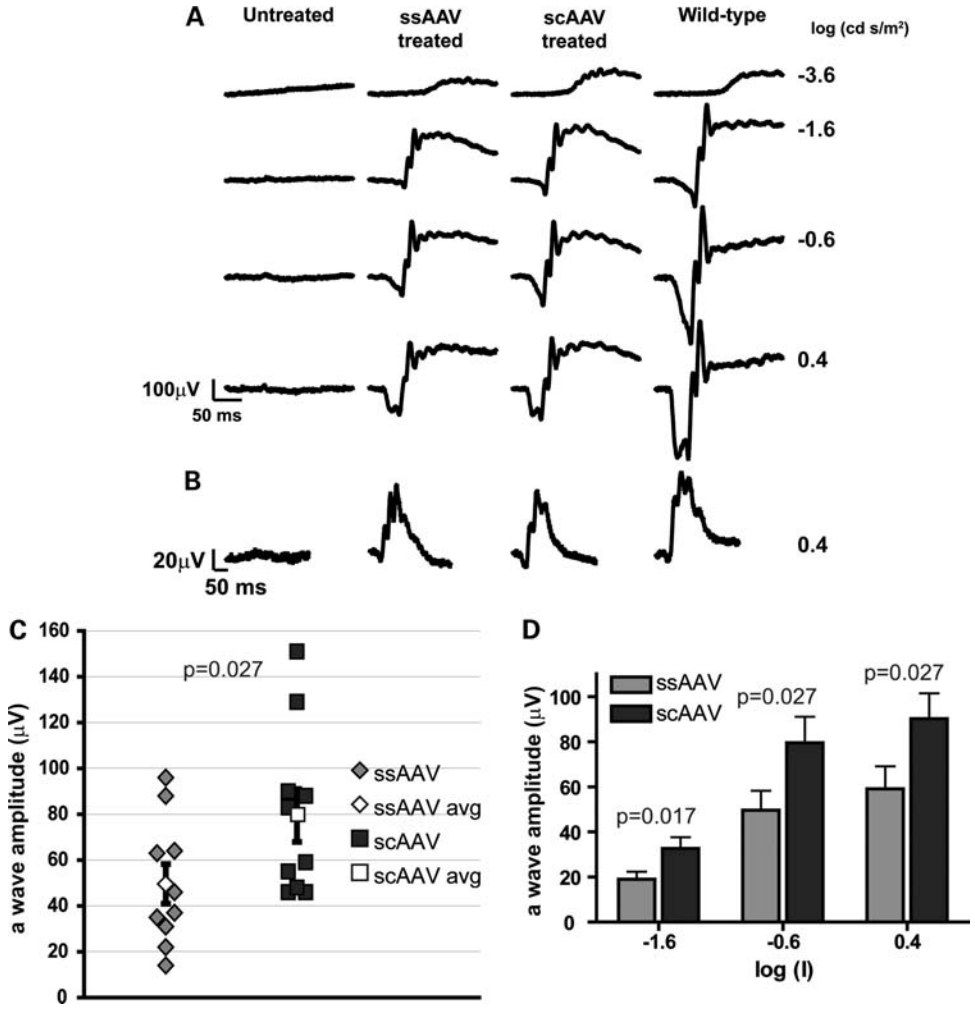

Figure 2. Light-dependent photoreceptor responses from *Aipl1*−/− mice following early AAV treatment. One eye of *Aipl1*−/− mice was injected at P2 with the indicated AAV and ERGs were recorded at P30. ERG responses from (**A**) dark- and (**B**) light-adapted conditions were measured at the indicated log (cd · s/m^2) flash intensities. Traces from a contralateral untreated eye and an age-matched wild-type mouse are shown for comparison. (**C**) Dark-adapted photoresponses from *Aipl1*−/− treated mice at the flash intensity of −0.6 (log cd s/m^2). Each data point represents the measured *a*-wave amplitude of an individual treated mouse. The group average of scAAV-treated mice was significantly higher than the group average of ssAAV-treated mice ($P \leq 0.027$). (**D**) Comparison of mean rod photoreceptor response (*a*-wave amplitude) between ssAAV and scAAV treatments over increasing flash intensities. Average *a*-wave amplitudes from the scAAV-treated mice were significantly greater than the ssAAV-treated mice at all intensities ($P \leq 0.027$). Error bars, ± SEM.

Early administration of AAV-mediated gene replacement therapy restores visually guided behavior in *Aipl1*−/− mice

To assess whether the observed rescue of electrophysiological responses and retinal morphology result in improvements in visually guided behavior, P2 AAV-treated mice were tested with the Morris water maze at P60. The Morris water maze, adapted from Pang *et al*. (48), tested for the ability of the mice to visually locate an escape platform. Under dim light conditions, untreated wild-type *Aipl1*+/+ mice took 3.45 ± 0.44 s ($n = 7$) to locate the platform (Fig. 5). In comparison, untreated *Aipl1*−/− mice located the platform in 24.09 ± 2.72 s ($n = 8$), which was significantly greater than wild-type mice ($P < 0.001$). *Aipl1*−/− mice treated with ssAAV found the platform in 6.88 ± 0.87 s ($n = 6$), and scAAV-treated mice took 7.82 ± 0.81 s ($n = 7$), both of which were significantly less than untreated *Aipl1*−/− mice ($P < 0.001$). There was no statistical difference between ssAAV-treated and wild-type mice, between scAAV-treated and wild-type mice, or between ssAAV- and scAAV-treated mice ($P > 0.05$ for all comparisons, analysis of variance (ANOVA) with Tukey–Kramer honestly significant difference (HSD) statistical analysis).

Gene replacement therapy with self-complementary AAV capsid mutant effectively rescues rod and cone function in *Aipl1*−/− mice with active photoreceptor degeneration

Our experiments comparing transduction kinetics of ssAAV and scAAV in wild-type retina demonstrated higher expression of AIPL1 at earlier time points with scAAV treatment. We hypothesized that this characteristic of scAAV is important in maximizing rescue of photoreceptors during active degeneration in *Aipl1*−/− mice, since these mice have a rapid

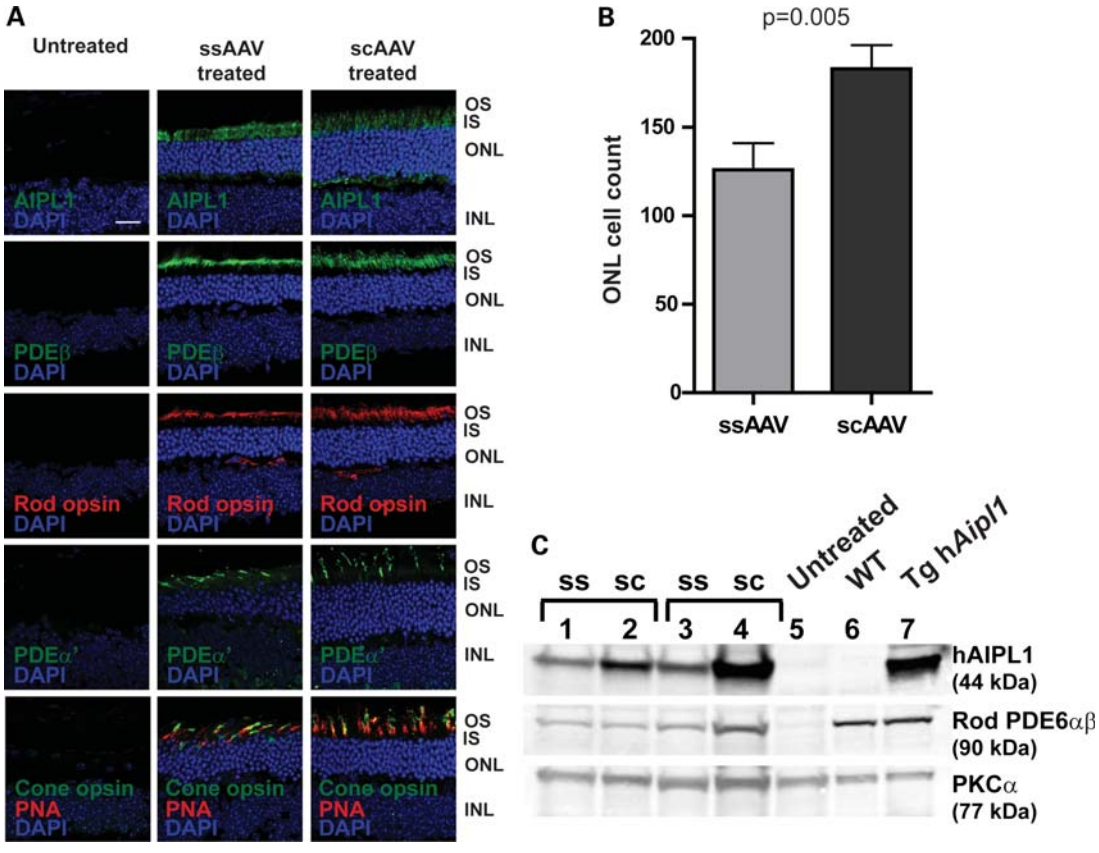

Figure 3. Restoration of photoreceptor morphology and PDE6 expression in *Aipl1*−/− retina following early AAV treatment. *Aipl1*−/− mice were treated at P2 and retinas were collected at P60 for immunocytochemistry and immunoblots. (**A**) Confocal images of retinal sections stained with indicated antibodies. Peanut agglutinin (PNA) (red) which stains the cone sheath is a cone marker. Cell nuclei were stained with DAPI (blue). Images were taken at ×63 magnification. Scale bar, 20 μm. OS, outer segment; IS, inner segment; ONL, outer nuclear layer; INL, inner nuclear layer. (**B**) Photoreceptor cell nuclei quantification of ssAAV- and scAAV-treated retina using retinal sections stained with DAPI. scAAV treatment showed significantly higher ONL cell counts than ssAAV-treated retina ($P \leq 0.005$). Error bars, ±SEM. (**C**) Western blots of retinal extracts from ssAAV- and scAAV-treated animals with indicated antibodies. Untreated *Aipl1*−/− (lane 5), wild-type (lane 6) and transgenic h*Aipl1* (lane 7) retina served as controls. PKCα expressed in bipolar cells, is a loading control.

rate of degeneration. To determine the efficiency of ssAAV and scAAV treatment in actively degenerating retina, viral injections were administered at P10. At this stage of retinal development, photoreceptor cell death is evident in *Aipl1*−/− mice (Supplementary Material, Fig. S1). ERG recordings were conducted at P30 to examine the effects of the delayed ssAAV and scAAV treatment on photoreceptor function. Representative ERG traces showed robust scotopic and photopic responses elicited from scAAV-treated animals compared with weak responses from ssAAV-treated animals (Fig. 6A and B). The photoreceptor response (*a*-wave amplitudes) of individual mice in each treatment group showed all scAAV-treated animals with higher *a*-wave amplitudes than ssAAV-treated animals, and a significant difference in group means ($P = 0.0006$; ssAAV treated mean = 4.22 ± 2.17 μV, $n = 9$; scAAV treated mean = 47.67 ± 10.73 μV, $n = 9$) (Fig. 6C), under dark-adapted conditions with a flash intensity of −0.6 log (cd s/m^2). Additionally, the difference in group means between ssAAV and scAAV treatment was significant for *a*-wave and *b*-wave amplitudes recorded under dark-adapted conditions, at all flash intensities of −3.6, −1.6, −0.6 and 0.4 log (cd s/m^2) (*P*-values indicated in figure, ranging from $P = 0.003$ to $P = 0.00001$) (Fig. 6D and E). A similar trend was observed with light-adapted ERG responses, a reflection of cone photoreceptor activity. A statistically significant difference in average *b*-wave amplitudes elicited under light-adapted conditions with a 0.4 log (cd s/m^2) flash intensity was observed ($P = 0.014$; ssAAV treated mean = 1.22 ± 1.22 μV, $n = 9$; scAAV treated mean = 20.44 ± 7.86 μV, $n = 9$) (Fig. 6F), with robust cone responses in scAAV-treated animals. While ERG responses of ssAAV-treated eyes were significantly lower than scAAV-treated eyes, they were significantly higher than contralateral untreated eyes at all flash intensities ($P < 0.05$) (data not shown).

Gene replacement therapy with self-complementary AAV capsid mutant slows rod and cone degeneration in *Aipl1*−/− mice with active photoreceptor degeneration

In P10 treated mice, the significant difference in ERG responses between ssAAV and scAAV already observed at P30 led us to conduct behavioral assays and morphological analyses at P35. Additionally, we wanted to accurately examine the behavioral and morphological correlates of the low ERG responses elicited from ssAAV-treated mice at P30. Morphological analyses were conducted to assess

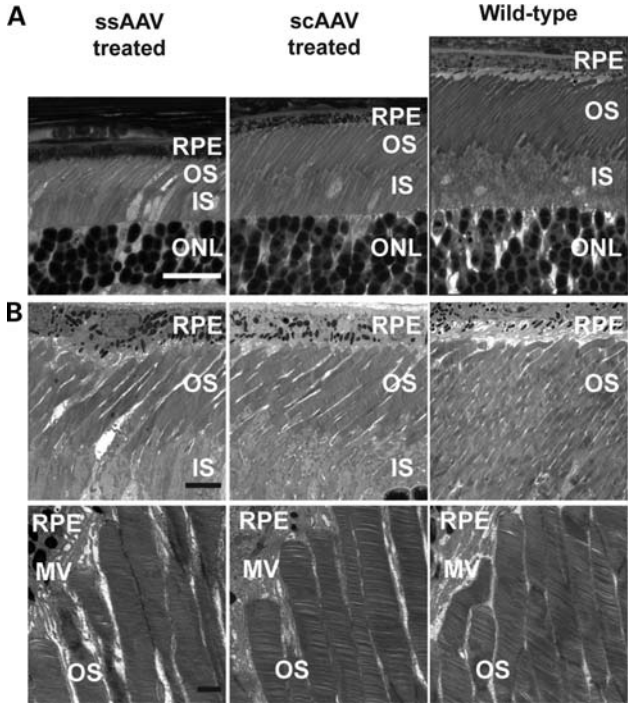

Figure 4. Restoration of photoreceptor ultrastructure following early AAV treatment. (**A**) Semithin light micrographs of P35 *Aipl1*−/− retina following treatment at P2 with ssAAV or scAAV. Semithin sections from a P35 *Aipl1*+/+ retina are shown for comparison. Scale bar, 20 μm. RPE, retinal pigmented epithelium; OS, outer segment; IS, inner segment; ONL, outer nuclear layer. (**B**) Electron micrographs at ×2200 (top panel) and ×8900 (bottom panel) magnification. RPE, retinal pigmented epithelium; MV, microvilli; OS, outer segment; IS, inner segment. Scale bars, 5 μm (top panel) and 1 μm (bottom panel).

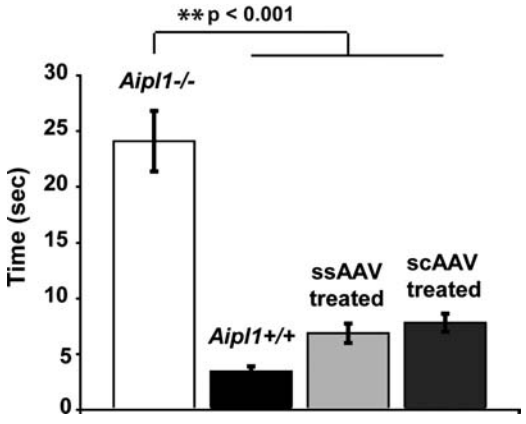

Figure 5. Vision-dependent behavior is restored in *Aipl1*−/− mice following early ssAAV or scAAV treatment. Mice received treatment at P2 and were tested at P60 with the Morris water maze. Age-matched untreated *Aipl1*−/− and *Aipl1*+/+ groups served as controls. The time to reach the escape platform was recorded and reported as group averages. Treatment with both AAVs restored vision-dependent behavior to wild-type *Aipl1*+/+ levels ($P > 0.05$), which were significantly different from untreated *Aipl1*−/− mice (**$P < 0.001$, ANOVA with Tukey–Kramer *post hoc* test). Error bars, ±SEM.

preservation of photoreceptors following delayed AAV-mediated gene replacement in *Aipl1*−/− mice at P10. Retina from scAAV-treated animals maintained five to six rows of photoreceptor cell nuclei (Fig. 7A, and Supplementary Material, Fig. S2). In comparison, retina from ssAAV-treated animals showed two to three rows of photoreceptor cell nuclei. These findings were supported by our cell counting results demonstrating the presence of significantly greater numbers of photoreceptor cell nuclei in retina from scAAV- than ssAAV-treated animals ($P = 0.0000001$; ssAAV mean = 76.90 ± 11.99; scAAV mean = 275.50 ± 21.71) (Fig. 7B).

Immunostaining for photoreceptor outer segment proteins such as rod and cone opsins revealed sparse and short outer segments in retina from ssAAV-treated animals, a pattern also observed with immunostaining for rod and cone PDE6 (Fig. 7A). In contrast, retina from animals treated with scAAV displayed denser and longer rod and cone outer segments (Fig. 7A). Coincident with the presence of photoreceptor outer segments, retina from animals treated with scAAV exhibited strong expression of AIPL1 in inner segments, and rod and cone PDE6 in respective photoreceptor outer segments (Fig. 7A). Our immunofluorescence results are supported by immunoblotting experiments demonstrating higher levels of hAIPL1 and rod PDE6 in the majority of retina from scAAV-treated animals (lanes 6–10) compared with ssAAV treated animals (lanes 1–5) (Fig. 7C). The amount of rod PDE6 in scAAV-treated retina varied from 10 to 40% of wild-type levels. In comparison, the amount of rod PDE6 in ssAAV-treated retinas was negligible, with 9% of wild-type rod PDE6 levels at best (lane 5).

Gene replacement therapy with self-complementary AAV capsid mutant rescues visually guided behavior in *Aipl1*−/− mice with active photoreceptor degeneration

To evaluate visually guided behavior following treatment at P10, mice were tested with the Morris water maze at P35 (Fig. 8). Similar to our previous results, *Aipl1*+/+ wild-type mice took 4.38 ± 0.45 s ($n = 6$) to locate the escape platform, whereas *Aipl1*−/− mice needed 25.20 ± 6.52 s ($n = 5$) ($P < 0.01$). ssAAV-treated mice took 24.00 ± 3.51 s ($n = 8$), which was significantly different from the wild-type ($P < 0.01$), but not from *Aipl1*−/− mice ($P > 0.05$). These results indicate that the visually guided behavior in P10 ssAAV-treated mice was not improved from untreated *Aipl1*−/− mice. In contrast, the average time of scAAV-treated mice to find the platform was 6.69 ± 1.30 s ($n = 7$), which was significantly less than ssAAV-treated mice and *Aipl1*−/− mice ($P < 0.01$), but not significantly different from *Aipl1*+/+ mice ($P > 0.05$), indicating that treatment with scAAV at P10 restored visually dependent behavior to wild-type levels. Similar results were observed when a comparison was conducted between ssAAV-treated mice demonstrating ERG responses and scAAV treated mice, where the average time of ssAAV-treated mice ($n = 4$, 17.87 ± 1.82 s) was significantly different than scAAV-treated mice ($n = 7$, 6.69 ± 1.30 s) ($P < 0.01$), but not significantly different from *Aipl1*−/− mice ($n = 5$, 25.20 ± 6.52 s) ($P > 0.05$) (ANOVA with Tukey–Kramer HSD statistical analysis).

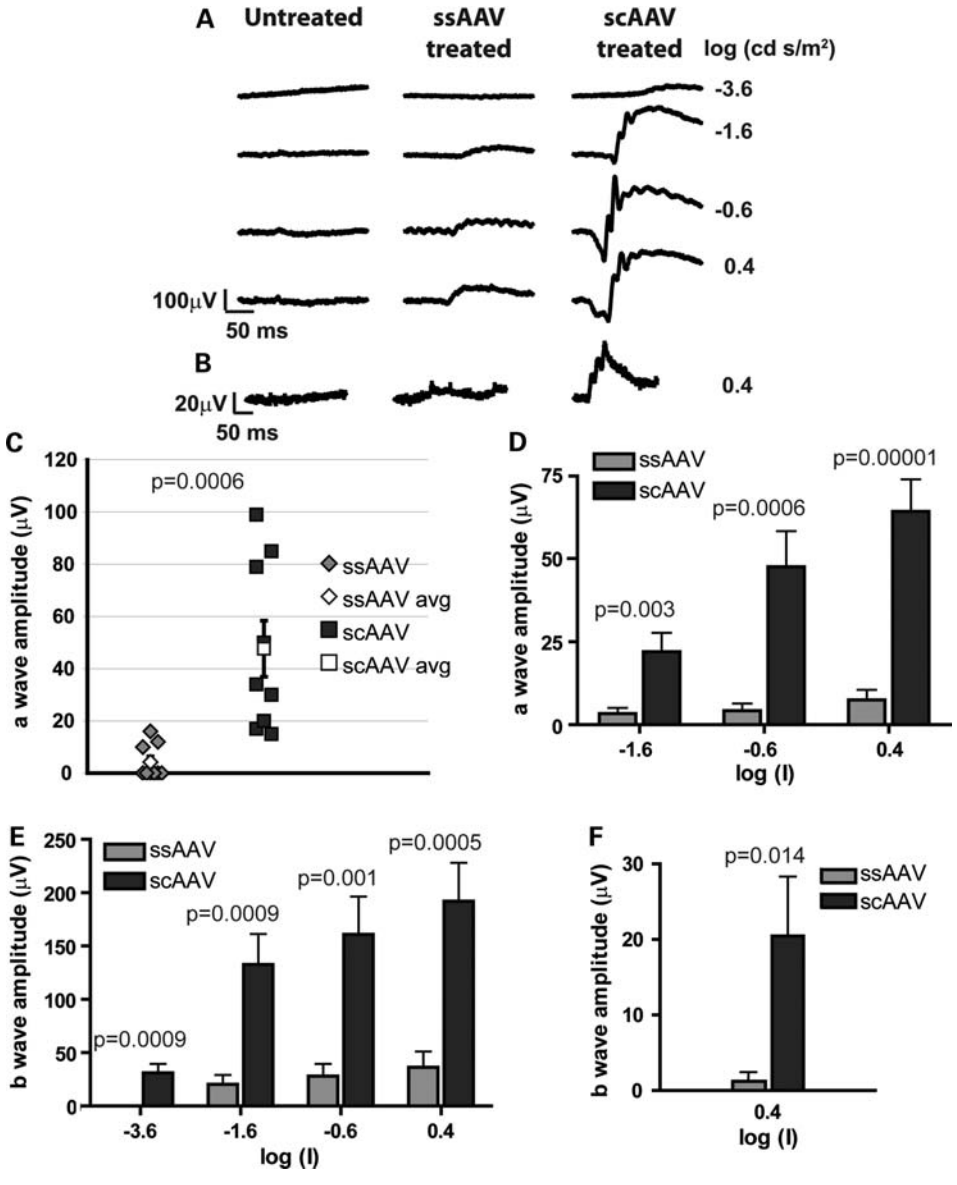

Figure 6. Light-dependent photoresponses in *Aipl1*−/− mice following late administration of AAV-mediated gene replacement therapy. ERG responses were recorded at P30, following injection at P10. ERG tracings were recorded under (**A**) dark-adapted and (**B**) light-adapted conditions at the indicated flash intensities. (**C**) *a*-wave amplitudes of individual mice in ssAAV- and scAAV-treated groups, derived from ERG recordings at −0.6 (log cd s/m^2) flash intensity. All scAAV-treated eyes showed higher *a*-wave amplitudes than ssAAV-treated eyes. Additionally, the group average of scAAV-treated mice was significantly higher than the group average of ssAAV-treated mice ($P \leq 0.0006$). Quantitative analysis of mean (**D**) *a*-wave and (**E**) *b*-wave amplitudes showed significantly higher amplitudes in the scAAV-treated group than the ssAAV-treated group across all flash intensities under dark-adapted conditions ($P \leq 0.003$). (**F**) Quantitative analysis of mean *b*-wave amplitudes from ERGs recorded under light-adapted conditions. Higher photopic responses were elicited from scAAV-treated eyes compared with ssAAV-treated eyes ($P \leq 0.014$). Error bars, ± SEM.

DISCUSSION

In this study, we demonstrated that the faster and greater transduction efficiency of sc-Y733F-AAV2/8 over ssAAV2/8 led to greater preservation of visual function in AAV-mediated gene replacement therapy of *Aipl1*-deficient mice, a model of severe LCA. This is the first reported study to use sc-Y733F-AAV2/8 for rescue of vision in a model of rapid retinal degeneration. Self-complementary AAV, shown to decrease expression latency and increase transduction efficiency, is generally thought to have limited use due to the halved gene packaging capacity of single-stranded AAV. However, it has been shown that efficient packaging and expression of genes up to 3.3 kb may be possible (49), extending the utility of self-complementary AAV. Additionally, the advent of capsid tyrosine mutations provides a simple way to increase viral efficiency without placing additional size restrictions. While mutations of surface-exposed tyrosine residues on viral capsids decrease ubiquitination which largely improves transduction efficiency, the effect on expression latency remains unclear.

Interestingly, we observed differences between ssAAV and sc-Y733F-AAV (scAAV) treatments in *Aipl1*−/− mice

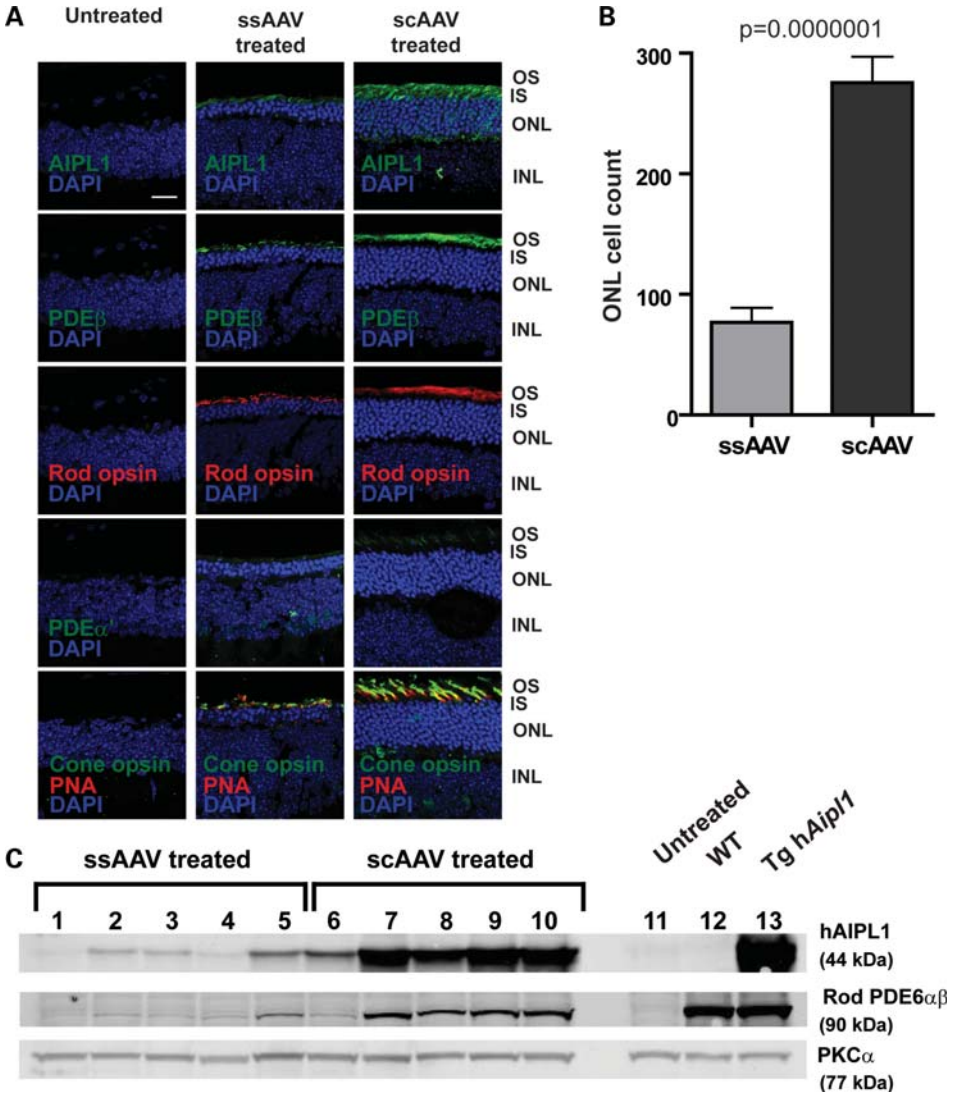

Figure 7. Photoreceptor morphology of *Aipl1*−/− retina following late administration of AAV-mediated gene replacement. *Aipl1*−/− mice were treated at P10 and retinas were collected at P35 for immunocytochemistry. (**A**) Confocal images of retinal sections stained with indicated antibodies. Peanut agglutinin (PNA) (red) is used as a cone marker. Cell nuclei are stained with DAPI (blue). Images were taken at ×63 magnification. Scale bar, 20 μm. OS, outer segment; IS, inner segment; ONL, outer nuclear layer; INL, inner nuclear layer. (**B**) Quantification of photoreceptor cell nuclei showed significantly greater nuclei in scAAV- compared with ssAAV-treated retina ($P \leq 0.0000001$). Error bars, ±SEM. (**C**) Western blots of ssAAV (lanes 1–5) and scAAV (lanes 6–10) treated retina. Untreated *Aipl1*−/− (lane 11), wild-type (lane 12) and transgenic h*Aipl1* (lane 13) retina serve as controls. PKCα expressed in bipolar cells, is a loading control.

treated at P2, when photoreceptors are not yet fully developed and no sign of degeneration is present. The aim of treating early was to provide maximal rescue of photoreceptors. Despite early treatment, we observed consistently lower ERG responses and photoreceptor cell survival in ssAAV-treated compared with scAAV-treated *Aipl1*−/− retina. However, the magnitude of differences between the two treatment groups did not translate into a difference in visually guided behavior under our lighting conditions. The observed differences between the two treatment groups were likely due to the lower levels of AIPL1 expression achieved with ssAAV, as demonstrated by our studies in wild-type retina. In contrast, the higher AIPL1 expression with scAAV treatment provided greater ERG responses and photoreceptor survival. In addition to these benefits in preservation of photoreceptor structure and function, viral vectors that achieve higher expression have a practical advantage, allowing for administration of lower viral titers which is especially important in reducing potential adverse effects. The use of the scAAV viral vector, therefore, may be warranted and beneficial in gene replacement therapy clinical trials.

The functional advantage of scAAV was most striking following P10 administration, when the *Aipl1*-deficient photoreceptors are undergoing active degeneration. Late treatment with ssAAV achieved minimal photoreceptor cell survival and low ERG responses in a fraction of the treated animals, with no evidence of vision guided behavior. In contrast, scAAV-treated animals showed greater photoreceptor cell survival, with concomitant ERG responses and vision guided behavior. Following late scAAV treatment, ERG responses

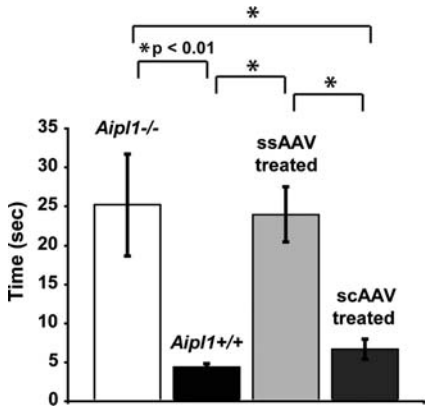

Figure 8. Vision-dependent behavior is restored to *Aipl1*−/− mice exclusively by scAAV treatment. Mice were tested at P35 after AAV administration at P10 with the Morris water maze assay. The mean time of scAAV-treated mice was similar to wild-type *Aipl1*+/+ mice ($P > 0.05$), and both were significantly lower than untreated *Aipl1*−/− and ssAAV-treated mice ($^*P < 0.01$ at group indicated comparisons, ANOVA with Tukey HSD). The mean time of ssAAV-treated mice was not significantly different from untreated *Aipl1*−/− mice ($P > 0.05$). Error bars, ±SEM.

persisted until the last time point tested at P60 (Supplementary Material, Fig. S4). The preservation of vision achieved with both early and late administration of scAAV treatment demonstrates stability of vision rescue. To summarize, in a clinically relevant scenario of active photoreceptor degeneration, scAAV treatment showed clear benefits over ssAAV in vision rescue.

The advantages in vision rescue with scAAV treatment were likely a result of the early robust expression of hAIPL1 observed in our comparisons of transduction efficiency in wild-type retina. It took an additional 3–4 days for expression levels of AIPL1 from ssAAV treatment to reach a level attained by that of scAAV treatment. We speculate that the faster expression of AIPL1 with scAAV translates into quicker restoration of functional PDE6 and stabilization of cGMP levels, and subsequently greater preservation of outer segments. This proved particularly critical in vision rescue in mice where photoreceptor degeneration has initiated. Additionally, the higher expression achieved with scAAV contributed to the improved vision rescue. It is known that *Aipl1* hypomorphic mice, which express 20–30% of wild-type AIPL1 levels, show abnormal photoreceptor function and slow degeneration (28). In contrast, *Aipl1* heterozygous mice, with 50% of protein, show no signs of photoreceptor degeneration or dysfunction (27). This indicates that a certain threshold level of AIPL1 is necessary for normal photoreceptor function and survival. The lower expression of AIPL1 achieved with ssAAV treatment in *Aipl1*−/− mice may lead to a number of photoreceptors that do not cross this threshold, resulting in lower photoreceptor survival and subsequent lower ERG responses. Higher AIPL1 expression levels achieved with scAAV treatment leads to a greater probability that this threshold is surpassed in a larger number of photoreceptors, hence achieving greater photoreceptor survival and restoration of vision.

The demonstrated functional advantages of second-generation AAV vectors, such as sc-Y733F-AAV2/8, are important in the future progress of AAV-mediated gene replacement therapy clinical trials. There is an impetus to broaden gene therapy clinical trials to treat a wider severity spectrum of inherited retinal dystrophies. Recent clinical studies report cases of adolescent and adult patients with genetic defects associated with rapid retinal degeneration, who show varying extents of ONL preservation and inner and outer segment integrity as observed with OCT. This has been observed in patients with defects in *CEP290* (50,51), *GUCY2D* (51), *RPGRIP1* (52) and *AIPL1* (34,35). These studies show that patients with genetic defects associated with rapid retinal degeneration may potentially benefit from AAV-mediated gene replacement therapy. The improved transduction onset and efficiency of second-generation AAV vectors, such as sc-Y733F-AAV2/8, provides a larger therapeutic range for treating a spectrum of genetic defects with varying rates of disease progression. Additionally, the longevity of such residual photoreceptors cannot be predicted for each patient, and the best practical option is to provide the most rapid acting and efficient treatment possible. It remains to be examined whether infants and young children afflicted with LCA have a substantial amount of photoreceptors that can be salvaged with early gene therapy treatment. The aim of gene therapy here would be prevention of massive loss of retinal neurons. Our results demonstrated that sc-Y733F-AAV2/8 also provided functional benefits over ssAAV2/8 in early treatment of rapid retinal degeneration. Additional concurrent progress in viral-mediated gene delivery and clinical characterization is necessary to advance into clinical trials, but emerging evidence in both areas shows promising prospects for gene replacement therapy to successfully treat a wider spectrum of genetic defects and severities of retinal dystrophies.

MATERIALS AND METHODS

Animals

Aipl1 knockout mice were generated and characterized previously (27). *Aipl1* knockout mice and wild-type used in this study are in a mixed C57Bl/129sv background. Mice were maintained under 12 h light/12 h dark light cycles. All experiments involving animals were approved by the Institutional Animal Care and Use Committee at West Virginia University.

Generation of recombinant AAV vectors

Full-length human *Aipl1* was amplified from human retinal cDNA using *Aipl1*-specific primers and cloned into the multiple cloning site of the parental pAAV-RKp-zsGreen vector to generate the pAAV-RKp-h*Aipl1* plasmid, which was used to produce the ssAAV2/8-RKp-h*Aipl1* viral vector as described in Sun *et al*. (37). RKp-h*Aipl1* was amplified from pAAV-RKp-h*Aipl1* with primers that engineered flanking *Kpn*I and *Eag*I sites, and cloned into the self-complementary AAV packaging vector, to generate the SC-RKp-h*Aipl1* plasmid. This plasmid was used to produce the scAAV2/8-Y733F-RKp-h*Aipl1* viral vector. The self-complementary-Y733F-AAV2/8 pseudotyped viral vector was generated as described previously, using the AAV8 capsid protein with Y733F surface-exposed tyrosine residue mutation

(43,53). All polymerase chain reaction amplifications were performed with Phusion GC DNA polymerase master mix (Finnymes, Thermo Scientific, Lafayette, CO, USA), following manufacturer instructions for cycling conditions. All plasmids were sequenced with the Big Dye Terminator ready reaction kit (Perkin Elmer, Waltham, MA, USA).

Subretinal injection

Aipl1−/− mice injected at P2 were anesthetized by chilling on ice. P10 *Aipl1*−/− mice and P14 wild-type mice were placed under general anesthesia with an intraperitoneal injection of ketamine (90 mg kg^{-1})/xylazine (9 mg kg^{-1}) and received a drop of dilation solution, consisting of a 1:1 mixture of tropicamide (1%, Alcon, Fort Worth, TX, USA): phenylephrine hydrochloride (2.5%, Bausch and Lomb, Tampa, FL, USA). For injection into mice prior to eyelid opening, an incision was made along the natural future eyelid line with surgical vannas scissors. A small incision was then made in the sclera just outside the pupillary margin with a 36-gauge needle. Viral solution was injected into the subretinal space using a pulled glass pipette attached to a pneumatic injector (MINJ-PD, Tritech Research, Los Angeles, CA, USA) using a transcorneal approach (54). Self-complementary and single-stranded AAV solutions were titer matched to 1.2×10^{13} viral particles per ml by diluting with phosphate buffered saline (PBS). Each animal received 1.0 μl of AAV in the right eye, and no injection in the untreated contralateral eye. Visualization during injection was aided by the addition of 0.1% fluorescein (100 mg ml^{-1} AK-FLUOR, Alcon) to the viral solutions.

Electroretinographic (ERG) analysis

Mice were dark-adapted overnight prior to testing. Eyes were topically dilated with a 1:1 mixture of tropicamide: phenylephrine hydrochloride. For ERG testing, mice were placed on a heated platform with continuous flow of isoflurane anesthesia through a nose cone (1.5% isoflurane in 2.5% oxygen). A reference electrode was placed subcutaneously in the scalp. ERG responses were recorded from both eyes with silver wire electrodes placed on each cornea, with contact being made with a drop of hypromellose solution (2% hypromellose in PBS) (Gonioscopic Prism Solution, Wilson Ophthalmic, Mustang, OK, USA). Rod dominated responses were elicited in the dark with flashes of LED white light at increasing flash intensities. Light-adapted cone responses were elicited in the presence of a 41 cd/m^2 rod desensitizing white background light with 2.5 cd s/m^2 LED white light flashes. ERGs were performed on the UTAS Visual Diagnostic System with BigShot Ganzfeld with UBA-4200 amplifier and interface, and EMWIN 9.0.0 software (LKC Technologies, Gaithersburg , MD, USA).

Vision-dependent behavioral assay

Morris water maze assay to test for visual dependent behavior was performed as described in Pang *et al*. (48). Mice were tested in a dim-lit room at 1.5 to 2.0 lux. Briefly, the task involved swimming in a 4 foot diameter water pool to an escape platform marked with a flag as a visual guidance cue. The time to reach the escape platform was recorded. The escape platform was washed between each trial to eliminate non-vision guided cues. Mice were trained to this task for 3 days, consisting of five trials each day. During this training period, the escape platform was stationary and the drop-off location of the mouse differed for each trial. On the fourth training day, the escape platform was moved to a different location in each trial. On the test day, day 5, the escape platform was also moved to a different location in each trial. However, to control for differences in swimming distances, the platform locations were kept constant for every mouse tested across all treatment groups. The reported times were taken from this final test day as group average times.

Immunoblotting, immunohistology and morphometric analysis

Mice were euthanized by CO_2 inhalation and eyes were enucleated. For immunoblots, flash frozen retinal samples dissected from enucleated eyes were sonicated in 6 M urea buffer (6 M urea, 4% sodium dodecyl sulfate (SDS), 0.5 M Tris pH 6.8, 10 mg/ml DTT). Protein concentrations were estimated using a NanoDrop spectrophotometer (Thermo Scientific). One hundred micrograms of total protein samples were resolved on 10% resolving SDS-polyacrylamide gel, and transferred onto polyvinylidene difluoride membranes (Immunobilon-FL, Millipore, Billerica, MA, USA). Membranes were blocked with blocking buffer (Rockland Inc., Gilbertsville, PA, USA) for 30 min at room temperature, and incubated with the indicated primary antibodies. Blots were washed in PBST (PBS, 137 mM NaCl, 2.7 mM KCl, 4.3 mM Na_2HPO_4 $7H_2O$, 1.4 mM KH_2PO_4, with 0.1% Tween-20) twice for 20 min and incubated in secondary antibody, goat anti-rabbit IRDye 680 (LI-COR Biosciences, Lincoln, NE, USA) for 30 min at room temperature. After three washes with PBST, membranes were scanned using the Odyssey Infrared Imaging System (LI-COR Biosciences), and bands quantified using Odyssey Infrared Imaging System software.

For immunohistochemical studies, eyes were immersed in 4% paraformaldehyde fixative for 15 min prior to removal of the anterior segments and lens. Eyecups were fixed for an additional 4 h, washed in PBS for 20 min, incubated in 10% sucrose/PBS for 1 h at room temperature and transferred to 20% sucrose/PBS for overnight incubation at 4°C. Eyes were then incubated in 1:1 mixture of 20% sucrose in PBS:OCT (Cryo Optimal Cutting Temperature Compound, Sakura, Torrance, CA, USA) for 1 h, and flash frozen in OCT. Cryosectioning was performed with a Leica CM1850 Cryostat, and serial retinal sections of 14 μm thickness were mounted on Superfrost Plus slides (Fisher Scientific, Pittsburgh, PA, USA). Retinal sections mounted on slides were washed with 1× PBSTx (1× PBS with 0.1% Triton X-100), and incubated for 1 h in blocking buffer (1× PBS with 5% goat sera, 0.5% Triton X-100, 0.05% sodium azide). Retinal sections were incubated with primary antibody for 2–3 h, followed by three 10 min washes with 1× PBSTx before incubation with secondary antibody (Alexa-Fluor 488 or Alexa-Fluor 568, Invitrogen, Carlesbad, CA, USA) for 30 min. The nuclear

marker, 4′,6-diamidino-2-phenylindole (DAPI, Invitrogen, 1:5000 dilution) was added for 10 min, and washed with 1× PBSTx before mounting with Prolong anti-fade reagent (Invitrogen) and cover slipping. Slides were viewed and imaged on a laser scanning confocal (Zeiss LSM 510) on a Zeiss LSM AxioImager Z1 microscope. Outer nuclear layer cell quantification was conducted on retinal sections from three different animals with the highest ERG responses in each treatment group. Serial sections for each retina were examined to determine the area with greatest photoreceptor preservation, which typically showed a uniform preservation in 40–50% of serial sections. Confocal images of DAPI-stained nuclei were taken at five fixed locations of a section, to control for variability across the eyecup. Confocal images were analyzed using ImageJ software (NIH, Bethesda, MD, USA) to determine the photoreceptor cell count, which was reported as an average of the 15 measurements. Each measurement spanned ∼200 μm in width of the retina.

For retinal whole mounts, eyes were enucleated with the orientation maintained by puncturing at the dorsal position, and fixed in 4% paraformaldehyde for 15 min. The anterior segments were removed to create an eyecup, and a vertical incision was created at the most dorsal position. The retina was carefully removed from the eyecup and fixed for an additional 6–12 h at 4°C. The retina was washed twice for 30 min prior to incubation in primary antibody for 12–24 h at 4°C. Removal of excess primary antibody was conducted with two 30 min washes, followed by incubation in secondary antibody for 12–24 h at 4°C, washed twice for 20 min and mounted and cover slipped. Whole mounts were viewed and imaged on an Olympus AX70 Provis microscope with an Optronics Microfire color CCD camera (Optronics, Golenta, CA, USA), using Stereo Investigator (MBF Bioscience, Milliston, VT, USA) and PictureFrame (Optronics) software. Quantification of whole mounts was conducted using ImageJ software to analyze 20× objective whole mount images taken with the same exposure time. Each data point, expressed in fluorescent arbitrary units, was an average of nine measurements obtained from three injected retinas with three images for each retina.

The following primary antibodies were used at the indicated dilutions: Human AIPL1 (1:1000) (27), PDE6αβγ (MOE) (1:2000) (CytoSignal Inc., Irvine, CA, USA), PDE6β (1:1000) (Affinity BioReagents, Golden, CO, USA), cone PDEα' (1:1000) (30), rod opsin (4D2) (1:2000) (gift from Dr Robert Molday, University of British Columbia, Vancouver, British Columbia, Canada), red/green opsin (1:1000) (Chemicon, Millipore, Billerica, MA, USA), PKCα (1:2000) (Thermo Fisher Scientific Inc., Pittsburgh, PA, USA). Rhodamine peanut agglutinin (PNA) (1:500) (Vector Laboratories, Inc, Burlingame, CA, USA) and DAPI (1:5000) (4′,6-diamidino-2-phenylindole, Invitrogen) were also used in immunocytochemistry.

Histologic, semithin sections and transmission electron microscopy

For hematoxylin and eosin stained images, enucleated whole eyes were fixed in Alcoholic Z-fix (Excalibur Pathology) for 48 h at room temperature. Serial sections of paraffin embedded fixed whole eyes were mounted on slides (Excalibur Pathology). Images were collected on an Olympus AX70 Provis microscope using PictureFrame software (Optronics).

For light and transmission electron microscopy, enucleated eyes were lightly fixed in freshly prepared fixative (2% paraformaldehyde, 2.5% glutaraldehyde, 0.1 M cacodylate buffer, pH 7.5) for 30 min. The anterior segment and lens were removed and eye cups were returned to fixative for 48 h at room temperature, prior to dissection into six to eight wedge-shaped pieces. Wedges were dehydrated in a graded ethanol series, then embedded in Polybed 812 (PolySciences, Inc.,Warrington, PA, USA). Semi-thin (1 μm) sections were collected onto glass slides, stained with toluidine blue and visualized using a Zeiss Axioimager 2 microscope equipped with EC Plan-Neofluar 40× (NA 0.75) and 100× (1.3 NA) objectives to identify best rescued areas. Thin sections (ca. 80 nm) from selected wedges were collected onto nickel grids, stained with 2% uranyl acetate and lead citrate and imaged using an FEI Morgagni transmission electron microscope at 80 kV.

Statistical analyses

Statistical analyses were conducted on GraphPad Prism4 software (GraphPad Software, Inc., La Jolla, CA, USA), using one-tailed unpaired *t*-tests for two group comparisons and ANOVA followed by Tukey–Kramer HSD *post hoc* tests for multiple group comparisons.

SUPPLEMENTARY MATERIAL

Supplementary materials are available on *HMG* online.

ACKNOWLEDGEMENTS

We thank the following people for their help and guidance with subretinal injection techniques: Dr Cristoforo Larzo at West Virginia University; Drs Constance Cepko and Takahiko Matsuda at Harvard University; and Drs Stephen Tsang and Nan-Kai Wang at Columbia University. We thank Dr Robert Molday at University of British Columbia, for generously providing the rod opsin (4D2) antibody. We thank Ms Loan Dang at Oakland University for her expertise in electron microscopy. We are grateful to Drs James O'Donnell and Hanting Zhang at West Virginia University for their help in establishing vision-dependent behavioral assay. Imaging experiments were performed in the West Virginia University Microscope Imaging Facility.

Conflict of Interest statement. W.W.H. and the University of Florida have a financial interest in the use of AAV therapies, and own equity in a company (AGTC Inc.) that might, in the future, commercialize some aspects of this work.

FUNDING

This work was supported by grants from National Institutes of Health (EY017035, EY11123, EY08571), West Virginia

Lions, Lions Club International Fund, Unrestricted Challenge Grant from Research to Prevent Blindness (RPB), Macular Vision Research Foundation, West Virginia University Center of Biomedical Research Excellence (COBRE) grants (RR016440) and West Virginia Graduate Student Fellowships in Science, Technology, Engineering, and Math (STEM) program.

REFERENCES

1. Daiger, S.P., Bowne, S.J. and Sullivan, L.S. (2007) Perspective on genes and mutations causing retinitis pigmentosa. *Arch. Ophthalmol.*, **125**, 151–158.
2. Schappert-Kimmijser, J., Henkes, H.E. and Van Den Bosch, J. (1959) Amaurosis congenita (Leber). *AMA Arch. Ophthalmol.*, **61**, 211–218.
3. Koenekoop, R.K. (2004) An overview of Leber congenital amaurosis: a model to understand human retinal development. *Surv. Ophthalmol.*, **49**, 379–398.
4. Foxman, S.G., Heckenlively, J.R., Bateman, J.B. and Wirtschafter, J.D. (1985) Classification of congenital and early onset retinitis pigmentosa. *Arch. Ophthalmol.*, **103**, 1502–1506.
5. Noble, K.G. and Carr, R.E. (1978) Leber's congenital amaurosis. A retrospective study of 33 cases and a histopathological study of one case. *Arch. Ophthalmol.*, **96**, 818–821.
6. Schroeder, R., Mets, M.B. and Maumenee, I.H. (1987) Leber's congenital amaurosis. Retrospective review of 43 cases and a new fundus finding in two cases. *Arch. Ophthalmol.*, **105**, 356–359.
7. Fulton, A.B., Hansen, R.M. and Mayer, D.L. (1996) Vision in Leber congenital amaurosis. *Arch. Ophthalmol.*, **114**, 698–703.
8. Perrault, I., Rozet, J.M., Gerber, S., Ghazi, I., Leowski, C., Ducroq, D., Souied, E., Dufier, J.L., Munnich, A. and Kaplan, J. (1999) Leber congenital amaurosis. *Mol. Genet. Metab.*, **68**, 200–208.
9. Hanein, S., Perrault, I., Gerber, S., Tanguy, G., Barbet, F., Ducroq, D., Calvas, P., Dollfus, H., Hamel, C., Lopponen, T. *et al.* (2004) Leber congenital amaurosis: comprehensive survey of the genetic heterogeneity, refinement of the clinical definition, and genotype-phenotype correlations as a strategy for molecular diagnosis. *Hum. Mutat.*, **23**, 306–317.
10. Galvin, J.A., Fishman, G.A., Stone, E.M. and Koenekoop, R.K. (2005) Evaluation of genotype-phenotype associations in leber congenital amaurosis. *Retina*, **25**, 919–929.
11. Redmond, T.M., Yu, S., Lee, E., Bok, D., Hamasaki, D., Chen, N., Goletz, P., Ma, J.X., Crouch, R.K. and Pfeifer, K. (1998) Rpe65 is necessary for production of 11-cis-vitamin A in the retinal visual cycle. *Nat. Genet.*, **20**, 344–351.
12. Pang, J.J., Chang, B., Hawes, N.L., Hurd, R.E., Davisson, M.T., Li, J., Noorwez, S.M., Malhotra, R., McDowell, J.H., Kaushal, S. *et al.* (2005) Retinal degeneration 12 (rd12): a new, spontaneously arising mouse model for human Leber congenital amaurosis (LCA). *Mol. Vis.*, **11**, 152–162.
13. Wrigstad, A., Narfstrom, K. and Nilsson, S.E. (1994) Slowly progressive changes of the retina and retinal pigment epithelium in Briard dogs with hereditary retinal dystrophy. A morphological study. *Doc. Ophthalmol.*, **87**, 337–354.
14. Chen, Y., Moiseyev, G., Takahashi, Y. and Ma, J.X. (2006) RPE65 gene delivery restores isomerohydrolase activity and prevents early cone loss in Rpe65−/− mice. *Invest. Ophthalmol. Vis. Sci.*, **47**, 1177–1184.
15. Bennicelli, J., Wright, J.F., Komaromy, A., Jacobs, J.B., Hauck, B., Zelenaia, O., Mingozzi, F., Hui, D., Chung, D., Rex, T.S. *et al.* (2008) Reversal of blindness in animal models of leber congenital amaurosis using optimized AAV2-mediated gene transfer. *Mol. Ther.*, **16**, 458–465.
16. Pang, J.J., Chang, B., Kumar, A., Nusinowitz, S., Noorwez, S.M., Li, J., Rani, A., Foster, T.C., Chiodo, V.A., Doyle, T. *et al.* (2006) Gene therapy restores vision-dependent behavior as well as retinal structure and function in a mouse model of RPE65 Leber congenital amaurosis. *Mol. Ther.*, **13**, 565–572.
17. Acland, G.M., Aguirre, G.D., Ray, J., Zhang, Q., Aleman, T.S., Cideciyan, A.V., Pearce-Kelling, S.E., Anand, V., Zeng, Y., Maguire, A.M. *et al.* (2001) Gene therapy restores vision in a canine model of childhood blindness. *Nat. Genet.*, **28**, 92–95.
18. Jacobson, S.G., Aleman, T.S., Cideciyan, A.V., Sumaroka, A., Schwartz, S.B., Windsor, E.A., Traboulsi, E.I., Heon, E., Pittler, S.J., Milam, A.H. *et al.* (2005) Identifying photoreceptors in blind eyes caused by RPE65 mutations: Prerequisite for human gene therapy success. *Proc. Natl Acad. Sci. USA*, **102**, 6177–6182.
19. Bainbridge, J.W., Smith, A.J., Barker, S.S., Robbie, S., Henderson, R., Balaggan, K., Viswanathan, A., Holder, G.E., Stockman, A., Tyler, N. *et al.* (2008) Effect of gene therapy on visual function in Leber's congenital amaurosis. *N. Engl. J. Med.*, **358**, 2231–2239.
20. Maguire, A.M., Simonelli, F., Pierce, E.A., Pugh, E.N. Jr, Mingozzi, F., Bennicelli, J., Banfi, S., Marshall, K.A., Testa, F., Surace, E.M. *et al.* (2008) Safety and efficacy of gene transfer for Leber's congenital amaurosis. *N. Engl. J. Med.*, **358**, 2240–2248.
21. Hauswirth, W.W., Aleman, T.S., Kaushal, S., Cideciyan, A.V., Schwartz, S.B., Wang, L., Conlon, T.J., Boye, S.L., Flotte, T.R., Byrne, B.J. *et al.* (2008) Treatment of leber congenital amaurosis due to RPE65 mutations by ocular subretinal injection of adeno-associated virus gene vector: short-term results of a phase I trial. *Hum. Gene Ther.*, **19**, 979–990.
22. Cideciyan, A.V., Aleman, T.S., Boye, S.L., Schwartz, S.B., Kaushal, S., Roman, A.J., Pang, J.J., Sumaroka, A., Windsor, E.A., Wilson, J.M. *et al.* (2008) Human gene therapy for RPE65 isomerase deficiency activates the retinoid cycle of vision but with slow rod kinetics. *Proc. Natl Acad. Sci. USA*, **105**, 15112–15117.
23. Cideciyan, A.V., Hauswirth, W.W., Aleman, T.S., Kaushal, S., Schwartz, S.B., Boye, S.L., Windsor, E.A., Conlon, T.J., Sumaroka, A., Pang, J.J. *et al.* (2009) Human RPE65 gene therapy for Leber congenital amaurosis: persistence of early visual improvements and safety at 1 year. *Hum. Gene Ther.*, **20**, 999–1004.
24. Simonelli, F., Maguire, A.M., Testa, F., Pierce, E.A., Mingozzi, F., Bennicelli, J.L., Rossi, S., Marshall, K., Banfi, S., Surace, E.M. *et al.* (2010) Gene therapy for Leber's congenital amaurosis is safe and effective through 1.5 years after vector administration. *Mol. Ther.*, **18**, 643–650.
25. Sohocki, M.M., Bowne, S.J., Sullivan, L.S., Blackshaw, S., Cepko, C.L., Payne, A.M., Bhattacharya, S.S., Khaliq, S., Qasim Mehdi, S., Birch, D.G. *et al.* (2000) Mutations in a new photoreceptor-pineal gene on 17p cause Leber congenital amaurosis. *Nat. Genet.*, **24**, 79–83.
26. Hendrickson, A., Bumsted-O'Brien, K., Natoli, R., Ramamurthy, V., Possin, D. and Provis, J. (2008) Rod photoreceptor differentiation in fetal and infant human retina. *Exp. Eye Res.*, **87**, 415–426.
27. Ramamurthy, V., Niemi, G.A., Reh, T.A. and Hurley, J.B. (2004) Leber congenital amaurosis linked to AIPL1: a mouse model reveals destabilization of cGMP phosphodiesterase. *Proc. Natl Acad. Sci. USA*, **101**, 13897–13902.
28. Liu, X., Bulgakov, O.V., Wen, X.H., Woodruff, M.L., Pawlyk, B., Yang, J., Fain, G.L., Sandberg, M.A., Makino, C.L. and Li, T. (2004) AIPL1, the protein that is defective in Leber congenital amaurosis, is essential for the biosynthesis of retinal rod cGMP phosphodiesterase. *Proc. Natl Acad. Sci. USA*, **101**, 13903–13908.
29. Kolandaivelu, S., Huang, J., Hurley, J.B. and Ramamurthy, V. (2009) AIPL1, a protein associated with childhood blindness, interacts with alpha-subunit of rod phosphodiesterase (PDE6) and is essential for its proper assembly. *J. Biol. Chem.*, **284**, 30853–30861.
30. Kirschman, L.T., Kolandaivelu, S., Frederick, J.M., Dang, L., Goldberg, A.F., Baehr, W. and Ramamurthy, V. (2010) The Leber congenital amaurosis protein, AIPL1, is needed for the viability and functioning of cone photoreceptor cells. *Hum. Mol. Genet.*, **19**, 1076–1087.
31. Sohocki, M.M., Perrault, I., Leroy, B.P., Payne, A.M., Dharmaraj, S., Bhattacharya, S.S., Kaplan, J., Maumenee, I.H., Koenekoop, R., Meire, F.M. *et al.* (2000) Prevalence of AIPL1 mutations in inherited retinal degenerative disease. *Mol. Genet. Metab.*, **70**, 142–150.
32. Simonelli, F., Ziviello, C., Testa, F., Rossi, S., Fazzi, E., Bianchi, P.E., Fossarello, M., Signorini, S., Bertone, C., Galantuomo, S. *et al.* (2007) Clinical and molecular genetics of Leber's congenital amaurosis: a multicenter study of Italian patients. *Invest. Ophthalmol. Vis. Sci.*, **48**, 4284–4290.
33. Walia, S., Fishman, G.A., Jacobson, S.G., Aleman, T.S., Koenekoop, R.K., Traboulsi, E.I., Weleber, R.G., Pennesi, M.E., Heon, E., Drack, A. *et al.* (2010) Visual acuity in patients with Leber's congenital amaurosis and early childhood-onset retinitis pigmentosa. *Ophthalmology*, **117**, 1190–1198.
34. Jacobson, S.G., Cideciyan, A.V., Aleman, T.S., Sumaroka, A., Roman, A.J., Swider, M., Schwartz, S.B., Banin, E. and Stone, E.M. (2011) Human retinal disease from AIPL1 gene mutations: foveal cone loss with minimal macular photoreceptors and rod function remaining. *Invest. Ophthalmol. Vis. Sci.*, **52**, 70–79.

35. Testa, F., Surace, E.M., Rossi, S., Marrocco, E., Gargiulo, A., Di Iorio, V., Ziviello, C., Nesti, A., Fecarotta, S., Bacci, M.L. *et al.* (2011) Evaluation of Italian patients with Leber congenital amaurosis due to AIPL1 mutations highlights the potential applicability of gene therapy. *Invest. Ophthalmol. Vis. Sci.*, **52**, 5618–5624.
36. Tan, M.H., Smith, A.J., Pawlyk, B., Xu, X., Liu, X., Bainbridge, J.B., Basche, M., McIntosh, J., Tran, H.V., Nathwani, A. *et al.* (2009) Gene therapy for retinitis pigmentosa and Leber congenital amaurosis caused by defects in AIPL1: effective rescue of mouse models of partial and complete Aipl1 deficiency using AAV2/2 and AAV2/8 vectors. *Hum. Mol. Genet.*, **18**, 2099–2114.
37. Sun, X., Pawlyk, B., Xu, X., Liu, X., Bulgakov, O.V., Adamian, M., Sandberg, M.A., Khani, S.C., Tan, M.H., Smith, A.J. *et al.* (2010) Gene therapy with a promoter targeting both rods and cones rescues retinal degeneration caused by AIPL1 mutations. *Gene Ther.*, **17**, 117–131.
38. McCarty, D.M., Monahan, P.E. and Samulski, R.J. (2001) Self-complementary recombinant adeno-associated virus (scAAV) vectors promote efficient transduction independently of DNA synthesis. *Gene Ther.*, **8**, 1248–1254.
39. Natkunarajah, M., Trittibach, P., McIntosh, J., Duran, Y., Barker, S.E., Smith, A.J., Nathwani, A.C. and Ali, R.R. (2008) Assessment of ocular transduction using single-stranded and self-complementary recombinant adeno-associated virus serotype 2/8. *Gene Ther.*, **15**, 463–467.
40. Petersen-Jones, S.M., Bartoe, J.T., Fischer, A.J., Scott, M., Boye, S.L., Chiodo, V. and Hauswirth, W.W. (2009) AAV retinal transduction in a large animal model species: comparison of a self-complementary AAV2/5 with a single-stranded AAV2/5 vector. *Mol. Vis.*, **15**, 1835–1842.
41. Kong, F., Li, W., Li, X., Zheng, Q., Dai, X., Zhou, X., Boye, S.L., Hauswirth, W.W., Qu, J. and Pang, J.J. (2010) Self-complementary AAV5 vector facilitates quicker transgene expression in photoreceptor and retinal pigment epithelial cells of normal mouse. *Exp. Eye Res.*, **90**, 546–554.
42. Zhong, L., Zhao, W., Wu, J., Li, B., Zolotukhin, S., Govindasamy, L., Agbandje-McKenna, M. and Srivastava, A. (2007) A dual role of EGFR protein tyrosine kinase signaling in ubiquitination of AAV2 capsids and viral second-strand DNA synthesis. *Mol. Ther.*, **15**, 1323–1330.
43. Zhong, L., Li, B., Mah, C.S., Govindasamy, L., Agbandje-McKenna, M., Cooper, M., Herzog, R.W., Zolotukhin, I., Warrington, K.H. Jr, Weigel-Van Aken, K.A. *et al.* (2008) Next generation of adeno-associated virus 2 vectors: point mutations in tyrosines lead to high-efficiency transduction at lower doses. *Proc. Natl Acad. Sci. USA*, **105**, 7827–7832.
44. Young, J.E., Vogt, T., Gross, K.W. and Khani, S.C. (2003) A short, highly active photoreceptor-specific enhancer/promoter region upstream of the human rhodopsin kinase gene. *Invest. Ophthalmol. Vis. Sci.*, **44**, 4076–4085.
45. Young, J.E., Gross, K.W. and Khani, S.C. (2005) Conserved structure and spatiotemporal function of the compact rhodopsin kinase (GRK1) enhancer/promoter. *Mol. Vis.*, **11**, 1041–1051.
46. Khani, S.C., Pawlyk, B.S., Bulgakov, O.V., Kasperek, E., Young, J.E., Adamian, M., Sun, X., Smith, A.J., Ali, R.R. and Li, T. (2007) AAV-mediated expression targeting of rod and cone photoreceptors with a human rhodopsin kinase promoter. *Invest. Ophthalmol. Vis. Sci.*, **48**, 3954–3961.
47. Dyer, M.A., Donovan, S.L., Zhang, J., Gray, J., Ortiz, A., Tenney, R., Kong, J., Allikmets, R. and Sohocki, M.M. (2004) Retinal degeneration in Aipl1-deficient mice: a new genetic model of Leber congenital amaurosis. *Brain Res. Mol. Brain Res.*, **132**, 208–220.
48. Pang, J.J., Boye, S.L., Kumar, A., Dinculescu, A., Deng, W., Li, J., Li, Q., Rani, A., Foster, T.C., Chang, B. *et al.* (2008) AAV-mediated gene therapy for retinal degeneration in the rd10 mouse containing a recessive PDEbeta mutation. *Invest. Ophthalmol. Vis. Sci.*, **49**, 4278–4283.
49. Wu, J., Zhao, W., Zhong, L., Han, Z., Li, B., Ma, W., Weigel-Kelley, K.A., Warrington, K.H. and Srivastava, A. (2007) Self-complementary recombinant adeno-associated viral vectors: packaging capacity and the role of rep proteins in vector purity. *Hum. Gene Ther.*, **18**, 171–182.
50. Cideciyan, A.V., Aleman, T.S., Jacobson, S.G., Khanna, H., Sumaroka, A., Aguirre, G.K., Schwartz, S.B., Windsor, E.A., He, S., Chang, B. *et al.* (2007) Centrosomal-ciliary gene CEP290/NPHP6 mutations result in blindness with unexpected sparing of photoreceptors and visual brain: implications for therapy of Leber congenital amaurosis. *Hum. Mutat.*, **28**, 1074–1083.
51. Pasadhika, S., Fishman, G.A., Stone, E.M., Lindeman, M., Zelkha, R., Lopez, I., Koenekoop, R.K. and Shahidi, M. (2010) Differential macular morphology in patients with RPE65-, CEP290-, GUCY2D-, and AIPL1-related Leber congenital amaurosis. *Invest. Ophthalmol. Vis. Sci.*, **51**, 2608–2614.
52. Jacobson, S.G., Cideciyan, A.V., Aleman, T.S., Sumaroka, A., Schwartz, S.B., Roman, A.J. and Stone, E.M. (2007) Leber congenital amaurosis caused by an RPGRIP1 mutation shows treatment potential. *Ophthalmology*, **114**, 895–898.
53. Zolotukhin, S., Potter, M., Zolotukhin, I., Sakai, Y., Loiler, S., Fraites, T.J. Jr, Chiodo, V.A., Phillipsberg, T., Muzyczka, N., Hauswirth, W.W. *et al.* (2002) Production and purification of serotype 1, 2, and 5 recombinant adeno-associated viral vectors. *Methods*, **28**, 158–167.
54. Matsuda, T. and Cepko, C.L. (2004) Electroporation and RNA interference in the rodent retina in vivo and in vitro. *Proc. Natl Acad. Sci. USA*, **101**, 16–22.